

## Effective Stress Analysis of Underground RC Structures during Earthquakes

Ming-wu WANG, Susumu IAI, Tetsuo TOBITA \*

\* Division of Geo-Hazards, Disaster Prevention Research Institute, Kyoto University

### Synopsis

Effective stress analyses are performed on seismic response of underground structures subjected to strong earthquake motions. The model of sand used for the analysis is based on the multiple shear mechanism. The seismic response data analyzed are based on the 30g centrifuge tests of an underground reinforced concrete (RC) box culvert, 9 m high and 12 m wide, buried at the bottom of saturated and dry model ground 16 m deep in prototype scale. Subject to a strong earthquake motion with a peak acceleration of 0.8 to 0.9g in prototype scale, earth pressures acting on the sidewalls of the RC structure increased after shaking in both saturated and dry model grounds. These earth pressures together with the effect of the lateral displacement due to shaking result in yielding of the side RC walls. The portion of the RC walls that are put into yielding is larger in saturated model ground than in dry model ground. The effective stress analyses are capable of capturing the essential features of the response of underground structures.

**Keywords:** centrifuge test, earth pressure, effective stress analysis, liquefaction, reinforced concrete (RC), underground structure, yield

### 1. Introduction

Seismic response of underground structures is a result of a complex soil-structure interaction. For a box culvert type structure, soil pushes one side wall if the soil displacement is larger than the structural displacement while soil pulls the other side of the wall. This is the case when the overall shear stiffness of a structure is stiffer than that of a corresponding soil column. In addition, soil above the top slab of a culvert causes lateral shear due to inertia force as well as vertical pressure due to gravity.

Seismic performance of underground RC structures has been studied successfully by experimental studies. Honda et al. (1999) performed static loading test on four cases of scaled box RC structures and evaluated cross sectional ductility of these structures. Aoyagi et al. (2001) studied the seismic performance of underground RC duct-type structures in dry sand. Koseki et al. (1997) and Kawashima (2000) studied the uplift behavior of underground structures in liquefiable soils based on case

histories, shaking table tests and centrifugal model tests. However, an analytical method to evaluate the performance of underground structures subjected to the complex soil-structure interaction described earlier has not been fully developed.

Analytical method based on the effective stress model, FLIP, is widely used to study seismic response of structures, especially those built in liquefiable soils (Iai et al., 1992). In this study, this analytical method is used to analyze the centrifuge test data on the seismic performances of underground RC structures. The centrifuge tests were performed for both dry and saturated model ground. The objective of this study is to investigate the applicability of this analytical method to simulate the response of underground RC structure subjected to the complex soil-structure interaction.

### 2. Centrifuge tests and numerical modeling

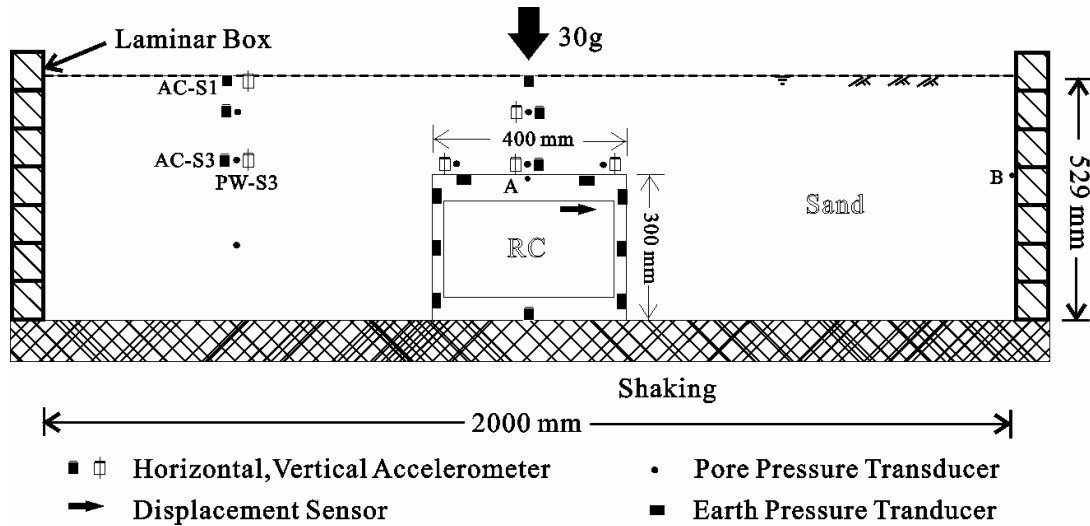


Fig. 1 Centrifuge test model

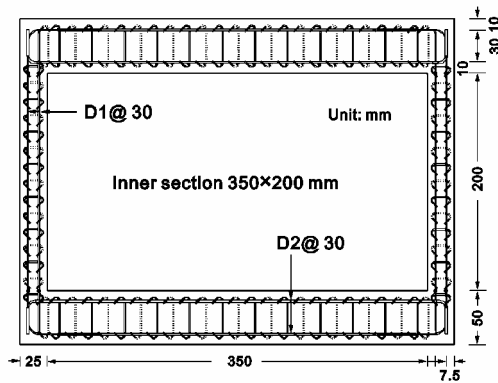


Fig. 2 Model RC structure

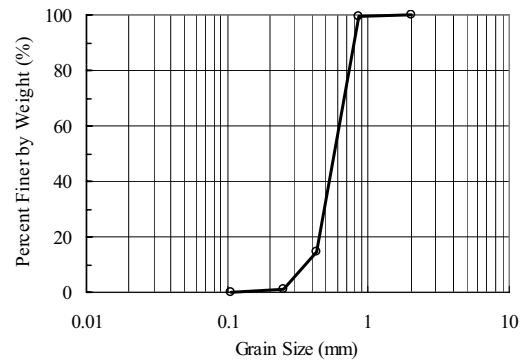


Fig. 3 Gradation curve of Silica No.7 sand

## 2.1 Centrifuge tests

The 30g centrifuge tests were performed in saturated and dry model ground. The centrifuge test model including instrumentation is shown in Fig. 1 for the saturated model ground. The test for dry model ground was similar to those shown in Fig. 1. A laminar shear box with internal dimensions of 2,000 (W) × 800 (L) × 600 mm (H) was used in the centrifuge tests. The model RC structure, shown in Fig. 2, had dimensions of 400 (W) × 250 (L) × 300 mm (H), in model scale. Thickness of sidewalls of model RC structures was 25 mm, thickness of the top and bottom slabs was 50 mm in model scale. The box culvert type RC structure was fixed to the base plate of the laminar shear box. Density, Young's modulus, and Poisson's ratio of model RC structure are 2.4 g/cm<sup>3</sup>, 2.33×10<sup>7</sup> kPa, and 0.2, respectively.

The soil profile consisted of an uniform Silica sand layer with a relative density of about 84%, about 15.67 m thick resting on stiff bedrock at prototype scale. Specific gravity, maximum and minimum void ratios of the sand are 2.684, 1.09 and 0.73, respectively. The grain size of sand is shown in Fig. 3. In saturated model ground, the soil is saturated with de-aired metolose solution, having 30 times the viscosity of water such that the deposit has the permeability of sand in prototype. The ground water level is shown in Fig. 1.

## 2.2 Numerical modeling

(1) Outline of effective stress analysis method, FLIP

A program FLIP (Finite element analysis program for Liquefaction Program) based on effective stress analysis method, developed by one of the authors (Iai et al., 1992), was used to analyze the seismic responses of

underground RC structures in this paper. The constitutive model used in the program is a model of multiple shear mechanism, originally proposed by Towhata and Ishihara (1985). The excess pore water pressure generation due to dilatancy is modeled using the concept of liquefaction front, as shown in Fig. 4, which is defined in the equivalent normalized stress space. In Fig. 4,  $S$  is a state variable,  $S = \sigma'_m / \sigma'_{mo}$ , under undrained condition with a constant total confining pressure, and  $r$  is the shear stress ratio,  $r = \tau_{mo} / \sigma'_{mo}$ . The program has been verified in many numerical simulation works of structure damage induced by earthquakes and liquefaction. The simulation using FLIP is done under two steps; static analysis and dynamic analysis. A static analysis is performed with gravity to simulate the initial stress acting in situ before the earthquake. Then a dynamic response analysis is done under undrained condition.

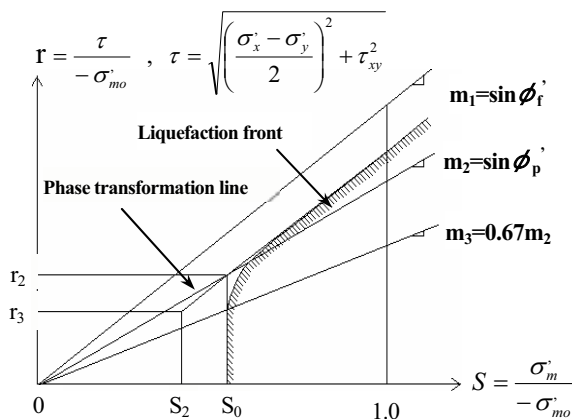


Fig.4 Schematic figure of liquefaction front (After Iai et al., 1992)

## (2) Simulation conditions and parameters

The finite element mesh used in the analysis is shown in Fig 5. The finite element model consists of 3,486 nodes and 6,532 elements. Horizontal slabs of RC structure are modeled with linear beam elements, and vertical sidewalls of RC structure are modeled with nonlinear (tri-linear) beam elements. To simulate the conditions of the centrifuge test using a laminar box, equal x-displacement and fixed boundaries are set up at the lateral and bottom boundaries, respectively, as shown in Fig.5. Slide along the interface between the sand and the RC structure was ignored in the analysis. The actual input motions measured on the base plate of the shaking table, shown in Fig. 6, were input to the bottom boundary of the analytical model. The saturated and dry model grounds are assumed to be of uniformly deposited sand of which density is  $1.942 \text{ g/cm}^3$  and  $1.501 \text{ g/cm}^3$ , respectively. The initial shear modulus of ground is 80,000 kPa, and hysteretic damping factor is 0.28 as shown in Fig. 7. The sand parameters for the simulation listed in the Table 1 are determined based on the laboratory tests and the simplified parameter identification method (Iai et al., 1990; Morita et al., 1997). More detailed definitions of model parameters may be found in the reference (Iai et al., 1992). The cyclic shear strength curves obtained by applying cyclic stress loading upon one element of the finite elements for the same sand, isotropically consolidated at the confined pressure of 98 kPa are shown in Fig. 8. The simulation results in the liquefaction when the shear stress ratio is 0.51 at 26 cycles of loading. The seismic response analysis was performed for the duration of 30 s with a time interval of 0.03s for the saturation model and 0.015 s for dry model, respectively. Wilson- $\theta$  method ( $\theta=1.4$ )

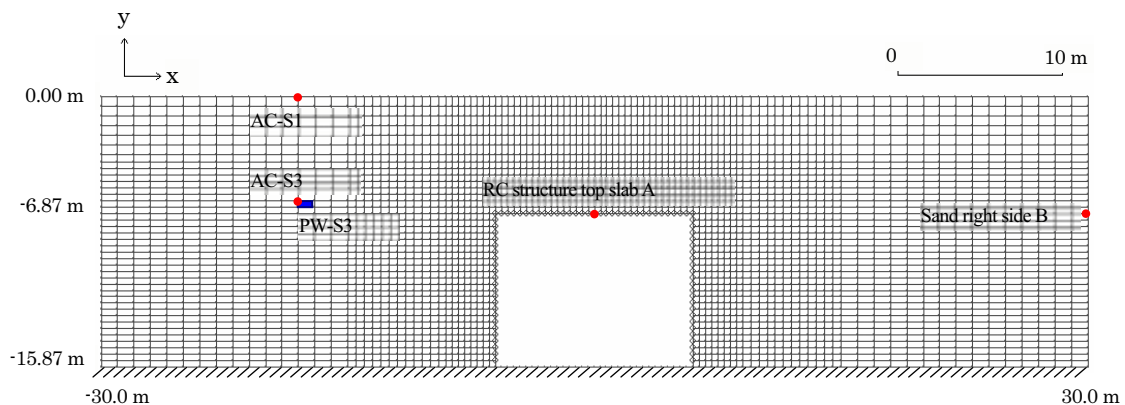


Fig. 5 Mesh, boundary, element type for numerical modeling

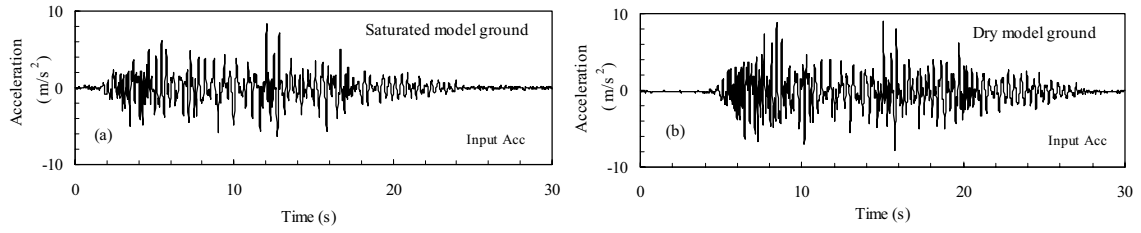


Fig. 6 Input motion for numerical simulation

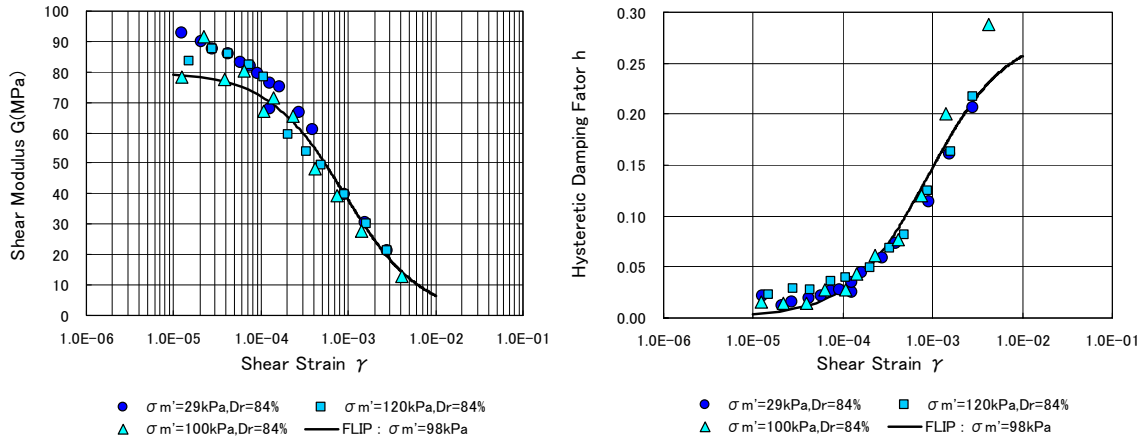


Fig. 7 Computed and measured strain dependent modulus and hysteretic damping

Table 1 Model parameters of the analysis of undrained cyclic loading

$K_{ma}$ (kPa)	$G_{ma}$ (kPa)	$\phi_f$ (°)	$h_{max}$	$\phi_p$ (°)	$S_1$	$p_1$	$p_2$	$w_1$	$c_1$
208600	80000	47	0.28	17	0.005	0.5	0.8	3.13	3.03

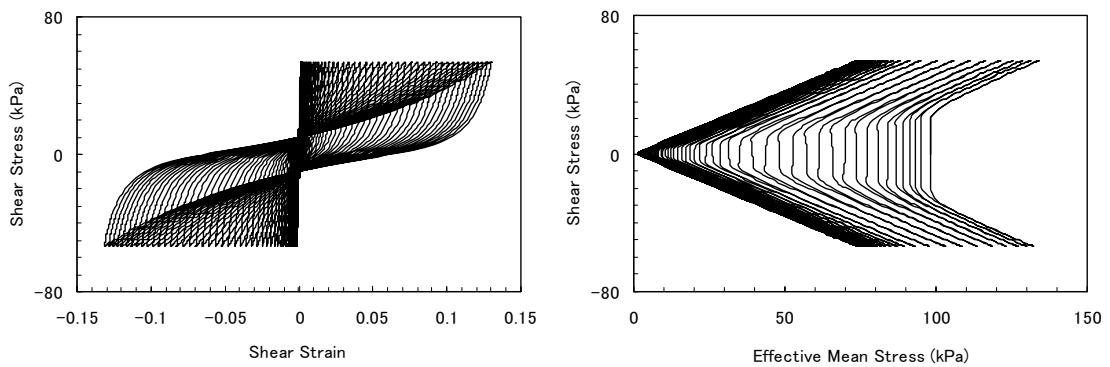


Fig. 8 Stress-strain curve and stress path obtained by numerical simulation of one sand element subjected to cyclic loading under undrained condition

was used with Rayleigh damping of  $\alpha=0.0$ ,  $\beta=0.002$  for numerical time integration.

### 3. Results and comparisons

#### 3.1 Results from centrifuge tests and simulations

##### (1) Saturated model ground

The underground RC model buried in saturated model ground was excited by a horizontal earthquake motion with a maximum acceleration of  $8.35 \text{ m/s}^2$  for a duration of 30s at prototype scale (Fig.6-a). The computed and measured time histories of displacements

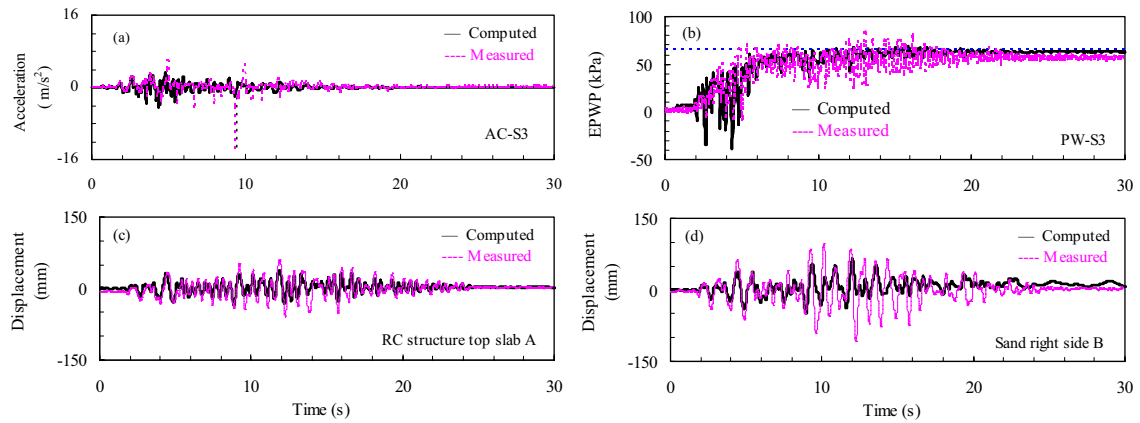


Fig. 9 Measured and computed response in saturated model ground

at the upper slab of RC structure, acceleration and excess pore water pressure of sand deposit are shown in Fig. 9. As mentioned earlier, the locations of instruments are indicated in Figs.1 and 5. The amplitude of acceleration at the ground decreased significantly after 6s of shaking (Fig. 9-a). The excess pore water pressure reached about 100% of initial effective vertical stress at 6s of shaking (Fig. 9-b). These facts suggest that the soil liquefied after 6s of shaking. The computed and measured acceleration and excess pore water pressures are in good agreement with each other.

Displacements at the top slab of RC structure and in ground at the same depth are shown in Figs. 9-c and 9-d. Both the computed and measured displacements in ground are larger than those at the top slab of RC structure. In particular, the computed and measured displacements at the top slab of RC structure agree with each other. However, the measured and computed displacements of lateral ground do not match with each other especially after 10s of shaking. There may be several reasons for this difference, including the effects of the laminar box for overall response of model ground. The most likely reason, however, is the stress-strain behavior of sand after liquefaction. The analysis model with the parameter used in this study behaves much stiffer manner than the centrifuge model ground.

As a whole, the analysis is able to capture the essential features of the response of the buried RC structure subject to a complex soil-structure interaction. Both the computed and measured results show that liquefaction occurred at 6s, causing de-amplification in acceleration. Both the computed and measure results show that displacement of ground is larger than that of RC structure.

These responses of soil and structure cause the change in lateral earth pressures acting on the side walls of the underground structure. Computed total normal stresses acting on the left sidewall, to be called earth pressures, are shown in Fig. 10 at three locations from the top to the bottom of the wall. The earth pressures during the centrifuge tests were not successfully measured. As shown in Fig. 10, the earth pressures gradually increased and reached, in average, the value of the total vertical stress in free field at 6s when the liquefaction occurred.

The computed and measured normal stresses applied

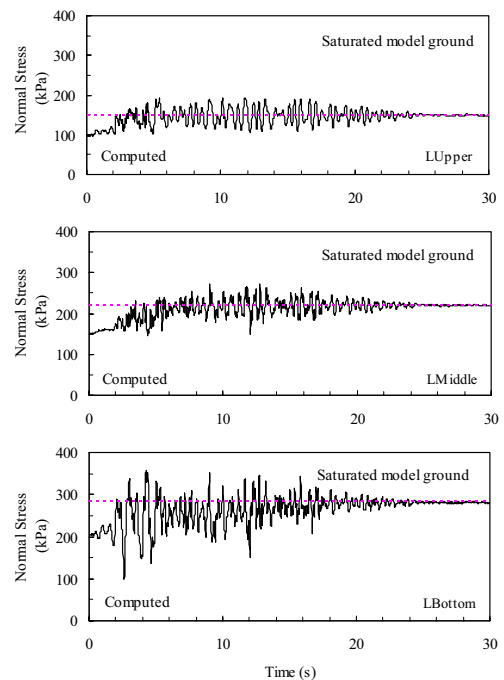


Fig. 10 Computed total normal stress acting on the left sidewall of RC structure in saturated model ground

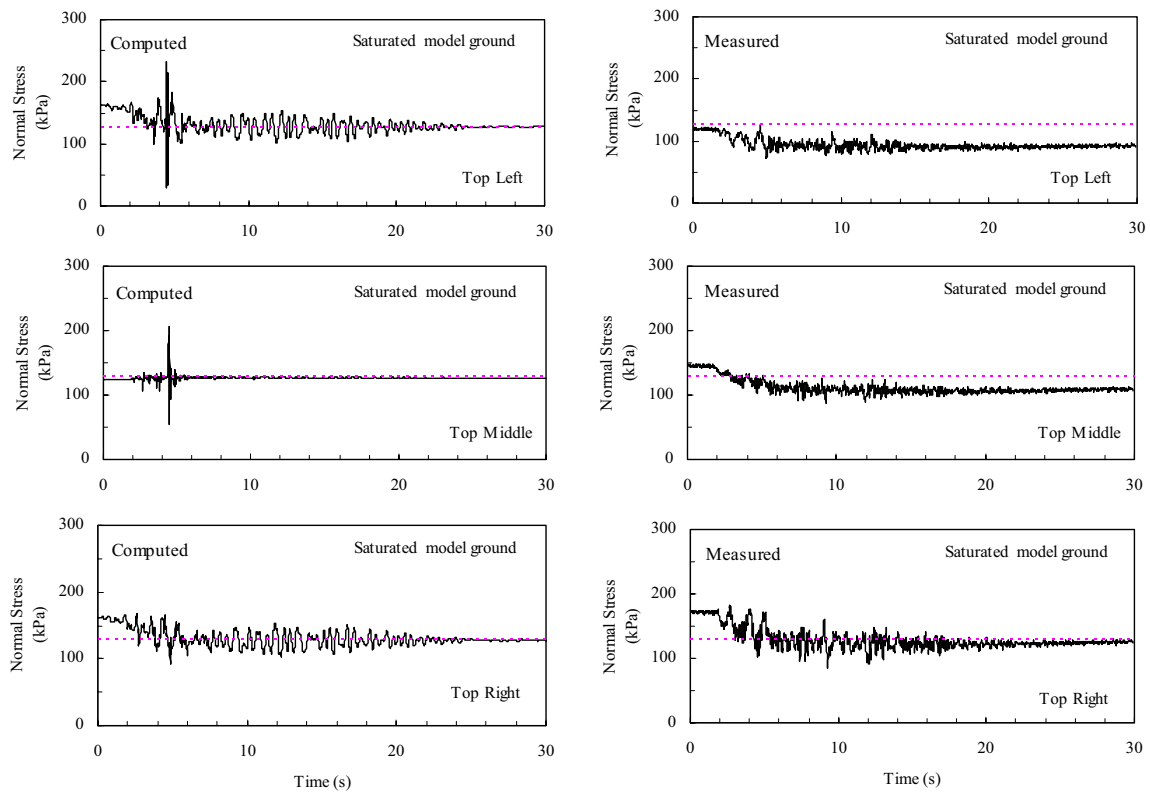


Fig. 11 Computed and measured normal stresses acting on the top slab of RC structure in saturated model ground

on the top slab of RC structure by the soil above it are shown in Fig. 11. The time histories shown are at the left corner, in the middle, and at the right corner of the top slab of the RC structure. The computed normal stresses at both corners of RC structure are initially larger than the total vertical stress at free field but gradually decreased and reached, in average, the value of the total vertical stress at free field. These changes are basically consistent with the change in the measured, except that the measured value at the left side was smaller by about 50kPa than that of the right side. The reason for this is not clearly known to the authors. The computed normal stress in the middle of the top slab of RC structure remained constant, in average, through the shaking whereas the measured one showed decreasing trend similar to those at both corners. The decreasing trend seen at both corners of the RC structure is presumed to be caused by the arching effect before shaking. This arching effect is caused by larger settlement of soil at the side of the wall than those of the top slab of the RC structure arising from the difference in overall stiffness of soil and RC structure in vertical direction. This arching effect may be sensitive to the preparation method of model ground, and thus caused the difference between

the computed and measured values in the middle of the top slab of RC structure.

## (2) Dry model ground

The underground RC model buried in dry model ground was excited by a horizontal earthquake motion with a maximum acceleration of  $9.06 \text{ m/s}^2$  for a duration of 30s at prototype scale (Fig. 6-b). The computed and measured time histories of acceleration and displacements at the upper slab of RC structure and at the ground are shown in Fig. 12. In contrast to the acceleration response of saturated model ground, amplitude of acceleration response in dry model ground did not decrease significantly during shaking (Fig. 12-a, b). The computed acceleration response agreed with those measured.

The computed displacement at the top slab of RC structure in dry model ground was almost identical with the ground displacement at the same depth (Fig. 12-c). This fact also applies to the measured displacement. However, the computed displacements were smaller than those measured. The reason for this is not clearly known to the authors.

These responses of soil and structure cause the

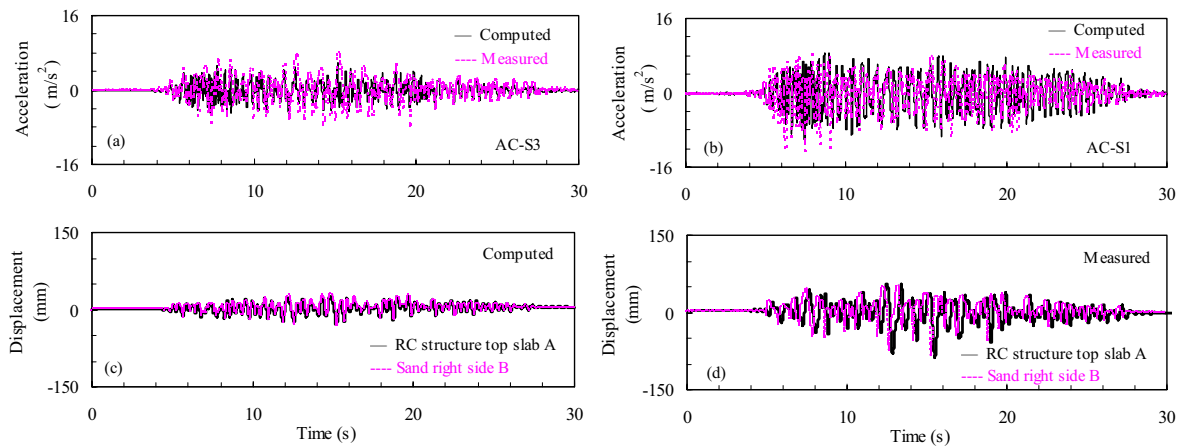


Fig. 12 Measured and computed response in dry model ground

change in lateral earth pressures acting on the side walls of the underground structure. Computed earth pressures acting on the left sidewall are shown in Fig. 13 at three locations from the top to the bottom of the wall. The earth pressures during the centrifuge tests were not successfully measured. As shown in Fig. 13, the earth pressures gradually increased but did not reach, in average, the value of the total vertical stress in free field at the mid height and bottom of the wall.

The computed and measured normal stresses applied on the top slab of RC structure by the soil above it are

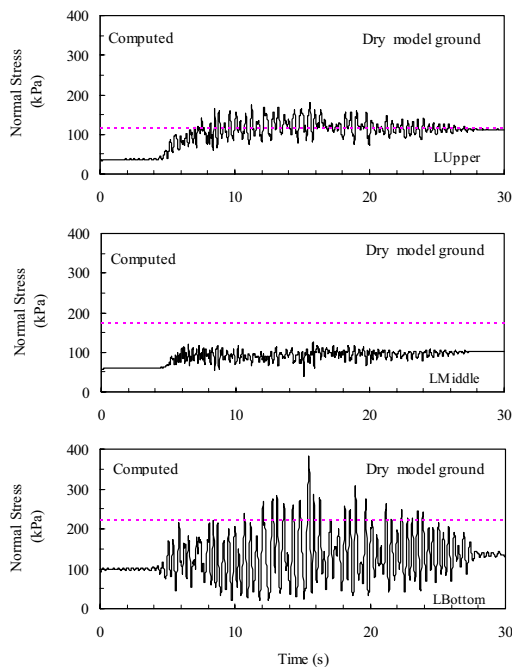


Fig. 13 Computed total normal stress acting on the left sidewall of RC structure in dry model ground

shown in Fig. 14. The time histories shown are at the left corner, in the middle, and at the right corner of the top slab of the RC structure. The computed normal stresses at both corners of RC structure are initially larger than the total vertical stress at free field but gradually decreased and becomes close to, in average, the value of the total vertical stress at free field. Measured normal stresses did not show significant change, in average, as those computed. As discussed in the case of saturated model ground, this arching effect may be sensitive to the preparation method of model ground, and thus caused the difference between the computed and measured values.

### 3.2 Comparison between responses of underground structure in saturated and dry model ground

The difference in the responses of ground and RC structure in saturated and dry model ground shown in the previous section causes difference in the earth pressures acting on the sidewall of RC structure depending on the model ground condition. As shown by broken lines in Fig. 15, the earth pressure distribution, in average, as represented by the residual values after shaking is generally larger in saturated model ground than in dry model ground. This may be because the soil in the saturated model ground reached the state of liquefaction, causing significant increase in earth pressures, whereas this is not the case for dry model ground. In addition, total vertical stress in saturated model ground, that is the value the earth pressure eventually reached in average, is larger than that in dry model ground. The earth pressure distribution at the time of maximum displacement at the top slab or RC structure, as shown by solid lines in Fig. 15, is larger for saturated model ground than for dry

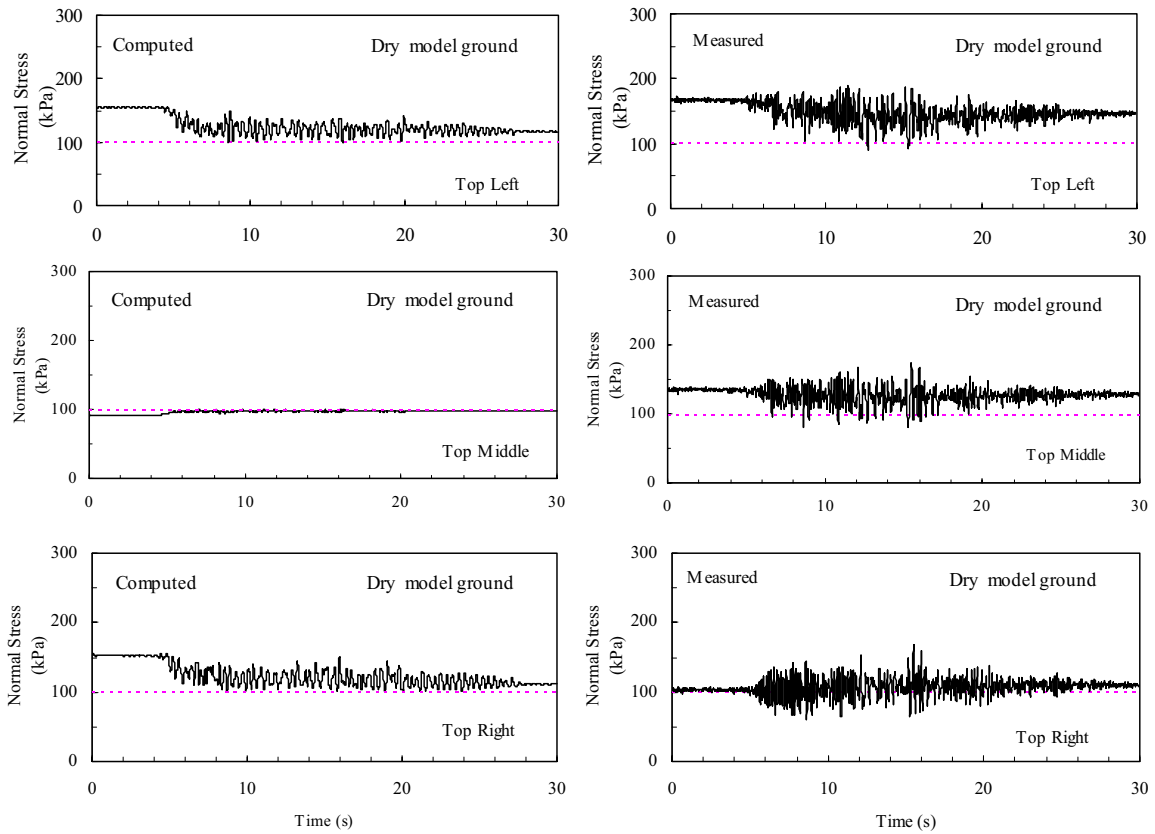


Fig. 14 Computed and measured normal stresses acting at the top slab of RC structure in dry model ground

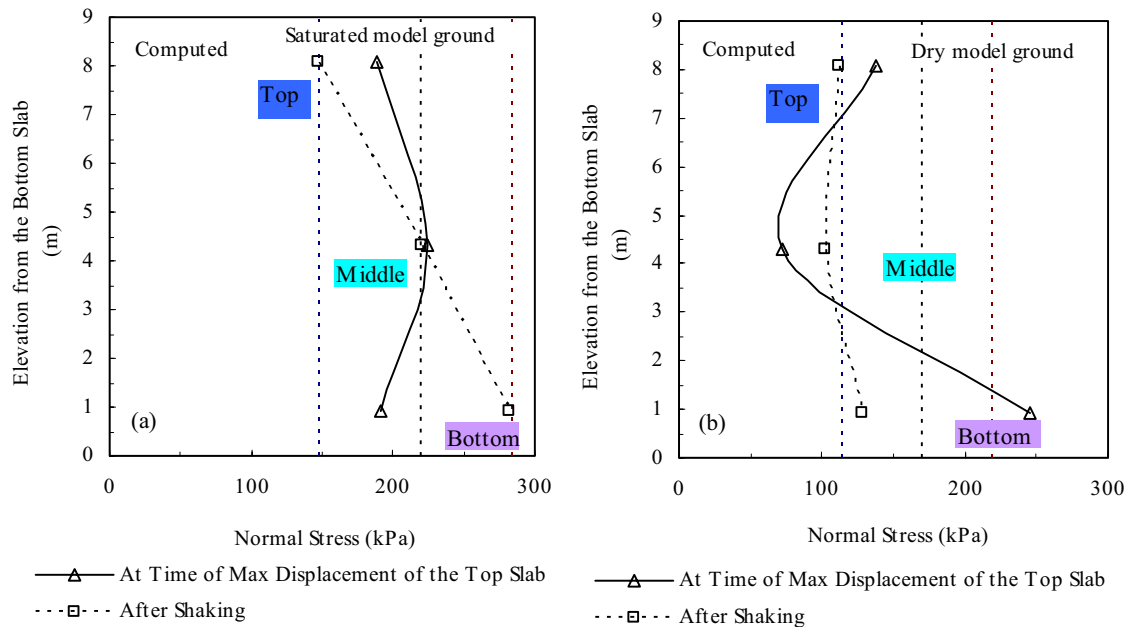


Fig. 15 Distribution of computed normal stresses acting on the left sidewall in saturated and dry model ground

model ground except for the bottom. This fact indicates that earth pressure distribution during shaking is much more complex than that after shaking. Instantaneous distribution of displacement in soil subject to complex

soil-structure interaction is presumed to govern these dynamic portions of earth pressure.

Fig. 16-a shows that the displacement of the left sidewall at time of maximum displacement of the top

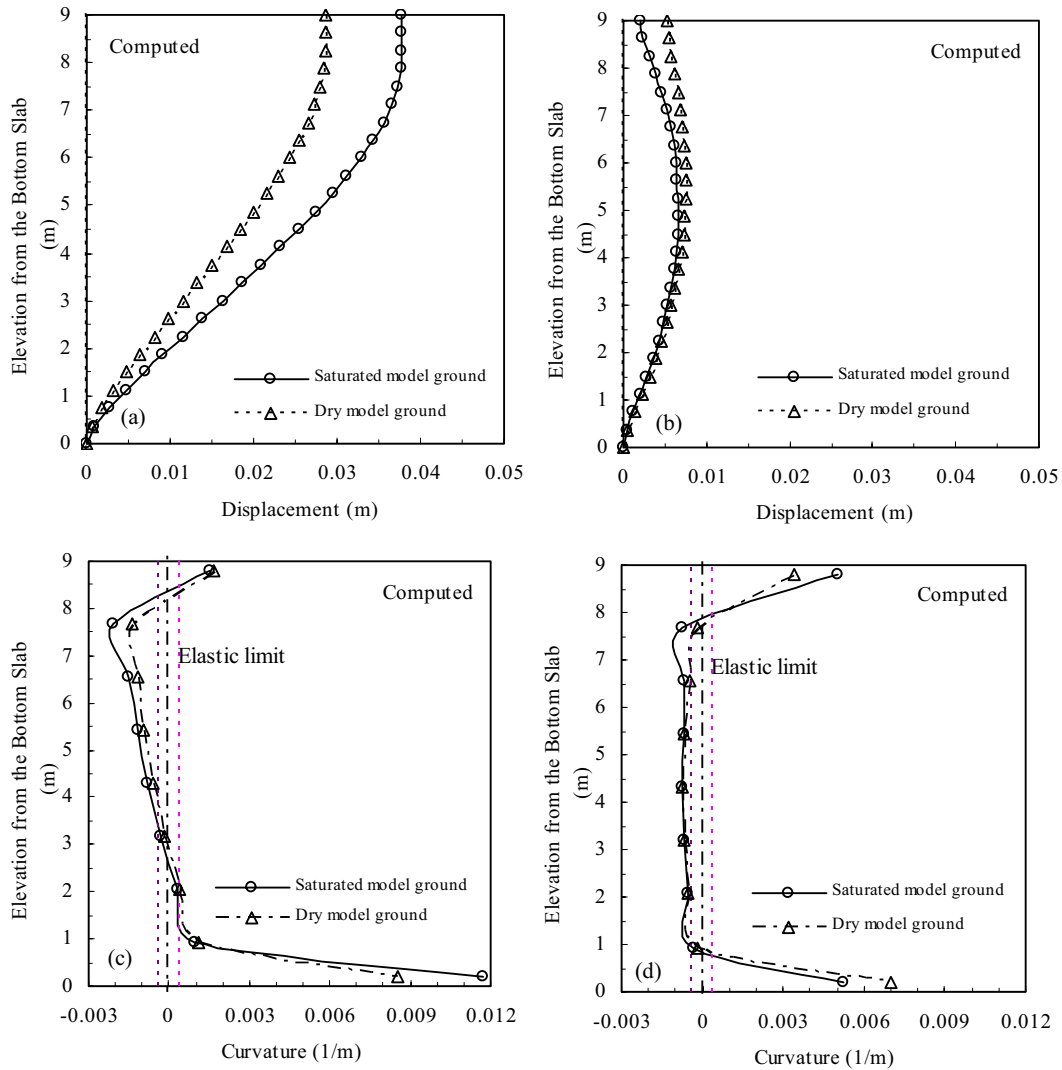


Fig. 16 Computed displacement and curvature of the left sidewall in saturated and dry model ground  
(a), (c): At time of maximum displacement of the top slab; (b), (d): After shaking

slab in saturated model ground is larger than that of dry model ground. However, their residual displacements are almost identical as shown in Fig. 16-b. Although there is a significant difference in the earth pressures in average for saturated and dry model ground, there is not a significant difference in the distribution of curvature of RC sidewall that is associated with inward deflection as shown in Fig. 16. The curvature at the maximum displacement at the top slab (Fig. 16-c) is associated with overall shear deformation of RC structure where as this is not the case for the residual after shaking (Fig. 16-d). The yielding associated with the peak response of RC structure may be the primary cause of the curvature distribution that was not significantly different in saturated and dry model ground.

In order to study the effect of soil-structure interaction based on the global shear deformation of RC

structure and ground in the vicinity, global shear strains

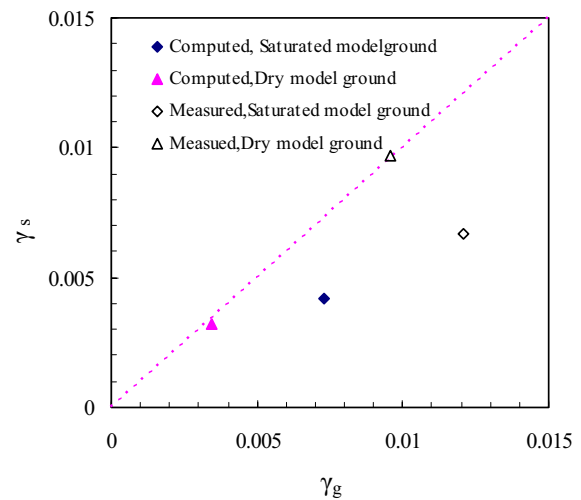


Fig. 17 Equivalent shear strain of whole structure  $\gamma_s$  and ground shear strain  $\gamma_g$

were computed based on the maximum relative displacement at the top slab of RC structure relative to the bottom and that at the same depth in the soil deposit. These global shear strains are shown in Fig. 17, where  $\gamma_s$  and  $\gamma_g$  denote the global shear strain of RC structure and ground, respectively. It may be seen that the value of  $\gamma_s$  and  $\gamma_g$  in dry model ground are almost identical with each other. This fact accords with the displacements discussed earlier. It is presumed that the dynamic earth pressures acting on the side wall may be small because the underground structure and ground deforms in a similar manner. However, earth pressures at the time of maximum displacement at the top slab of RC structure are significantly different from those after shaking as shown in Fig. 15. Displacement of soil in the ground is presumed to be much more complex than those assumed as linear distribution along depth.

In saturated model ground, the global shear strain of RC structure is less than that of ground. This leads to a thought that the earth pressures at the time of maximum displacement at the top slab of RC structure is larger than those after shaking. However, this was not the case as shown in Fig. 15. Once again, displacement of soil in the ground is presumed to be much more complex than those assumed as linear distribution along depth.

#### 4. Conclusions

Based on the effective stress analysis performed in this study combined with centrifuge test data, the following conclusions are obtained with respect to the seismic performance of underground RC structures.

- 1) Lateral displacement of ground is larger than that of RC structure in saturated model ground. These displacements are almost identical with each other in dry model ground.
- 2) Computed plastic yielding region of RC structures and earth pressures in saturated model ground are larger than those in dry model ground. This result is consistent with the cracks observed in RC structures during centrifuge tests.
- 3) Earth pressures acting on the sidewalls of RC structures increased during shaking both in saturated and dry model ground, gradually approaching, in average, the total vertical stress in free field.
- 4) Computed earth pressures acting on the top slab decreased and, in average, reached to the total vertical stress in free field. Similar trend was recognized in

centrifuge tests. This may be due to the arching effects before shaking.

- 5) The effective stress analysis performed in this study is capable of capturing the essential features of the response of underground structures discussed in 1) through 4).

#### Acknowledgements

This research has been supported by nine Japanese power companies and Japan Atomic Power Co. through the grant for Joint Research Program "An advanced study on the evaluation method of seismic safety of underground reinforced concrete structures in nuclear power plants", 2003-2005.

#### References

- Aoyagi, Y., Kanazu, T., Endoh, T. and OKaichi, A. (2001): Research on streamlining seismic safety evaluation of underground reinforced concrete duct-type structures in nuclear power stations-part-1 scope, objectives and major results of the research. Transactions of the 16th International Conference on Structural Mechanics in Reactor Technology, Division K, paper number 1295.
- Honda, K., Adachi, M., Ishikawa, H. and Hasegawa, T. (1999): Experimental study on deformational property of box culvert subjected to lateral Load. Proceedings of the Japan Concrete Institute, Vol. 21, No. 3, pp. 1261-1266.
- Iai, S., Matsunaga, Y., Kameoka, T. (1992): Strain space plasticity model for cyclic mobility. Soils and Foundations, Vol. 32, No. 2, pp. 1-15.
- Iai, S., Matsunaga Y., Kameoka. T. (1990): Parameter identification for a cyclic mobility model. Rep Port Harbour Res Inst, Vol. 29, No. 4, pp. 57-83.
- Kawashima, K. (2000): Seismic design of underground structures in soft ground: A review. Geotechnical Aspects of Underground Structures in Soft Ground, Balkema, pp. 3-19.
- Koseki, J., Matsuo, O. and Koga, Y. (1997): Uplift behavior of underground structures caused by liquefaction of surrounding soil during earthquake. Soils and Foundations, Vol. 37, No.1, pp. 97-108.
- Morita, T., Iai, S., Liu, H. and et al. (1997): Simplified method to determine parameter of FLIP. Technical Note of the Port and Harbour Research Institute

Ministry of Transport, No. 869. (in Japanese)  
Ozutsumi, O., Sawada, S., Iai, S. and et al. (2002):  
Effective stress analysis of liquefaction-induced  
deformation in river dikes. Soil Dynamics and  
Earthquake Engineering, Vol. 22, No. 9-12, pp.  
1075-1082.

Towhata, I., Ishihara, K. (1985): Modelling soil  
behaviour under principal stress axes rotation,  
Proceedings of the Fifth International Conference on  
Numerical Methods in Geomechanics, Vol. 1, pp.  
523-530.

## 地震時の地下RC構造物の有効応力解析

汪 明武・井合 進・飛田哲男

### 要旨

地下構造物の地震時挙動を、多重せん断機構に基づく砂の力学モデルに基づいて有効応力解析した。解析対象は、矩形断面の鉄筋コンクリート製（RC）が飽和および乾燥地盤の基盤に埋設されたもので、30g場での遠心実験に基づく。地震動加振の結果、RC構造物の側壁に作用する土圧は加振とともに増加し、RC構造物の側壁は降伏に至った。有効応力解析の結果は、RC構造物の地震時挙動をよく説明するものとなった。

**キーワード:**遠心力載荷実験, 土圧, 有効応力解析, 液状化, 鉄筋コンクリート（RC）, 地下構造物, 降伏

